*Int. J. Appl. Math. Comput. Sci.*, 2008, Vol. 18, No. 3, 399–407
DOI: 10.2478/v10006-008-0036-5

# AN AUTOMATIC HYBRID METHOD FOR RETINAL BLOOD VESSEL EXTRACTION

YONG YANG [*,**], SHUYING HUANG [***], NINI RAO [*]

[*] School of Life Science and Technology
University of Electronic Science and Technology of China, Chengdu 610054, P. R. China
e-mail: {greatyyy765,hitli}@sohu.com

[**] School of Information Management
Jiangxi University of Finance and Economics, Nanchang 330013, P. R. China
e-mail: greatyang@mail.xjtu.edu.cn

[***] School of Electronics
Jiangxi University of Finance and Economics, Nanchang 330013, P. R. China
e-mail: greathsy@sohu.com

The extraction of blood vessels from retinal images is an important and challenging task in medical analysis and diagnosis. This paper presents a novel hybrid automatic approach for the extraction of retinal image vessels. The method consists in the application of mathematical morphology and a fuzzy clustering algorithm followed by a purification procedure. In mathematical morphology, the retinal image is smoothed and strengthened so that the blood vessels are enhanced and the background information is suppressed. The fuzzy clustering algorithm is then employed to the previous enhanced image for segmentation. After the fuzzy segmentation, a purification procedure is used to reduce the weak edges and noise, and the final results of the blood vessels are consequently achieved. The performance of the proposed method is compared with some existing segmentation methods and hand-labeled segmentations. The approach has been tested on a series of retinal images, and experimental results show that our technique is promising and effective.

**Keywords:** blood vessel extraction, retinal image, mathematical morphology, fuzzy clustering.

## 1. Introduction

Retinal images of humans play an important role in the detection and diagnosis of many eye diseases for ophthalmologists (Rawi *et al.*, 2007). Some diseases such as glaucoma (Stapor *et al.*, 2004; Stapor and Switonski, 2004), diabetic retinopathy, and macular degeneration are very serious for they can lead to blindness if they are not detected in time and correctly (Riveron and Guimeras, 2006). Therefore, automatic detection for retinal images is necessary, and among them the detection of blood vessels is most important. The information about blood vessels, such as length, width, tortuosity and branching pattern, can not only provide information on pathological changes but can also help to grade diseases severity or automatically diagnose the diseases (Chanwimaluang and Fan, 2003). However, manual detection of blood vessels is much more difficult since the blood vessels in a retinal image are complex and with low contrast. In addition, there are usually a number of retinal images to judge a disease. Hence, a manual measurement becomes tiresome. As a result, reliable and automatic methods for extracting and measuring the vessels in retinal images are needed.

In the past years, many approaches for extracting retinal image vessels have been developed and applied. The matched filter approach is a widely used template-based method, which was firstly proposed by Chaudhuri *et al.* (1989) and further extended by Hoover *et al.* (2000). This method usually uses a two-dimensional linear structural element that has a Gaussian cross-profile section, extruded or rotated into three dimensions to identify the cross-profile of the blood vessels. The resulted image is finally thresholded to produce a binary segmentation of the vasculature. However, with this method in the detected images, the junction points are not always detected, small ves-

sels are missed and the validity of the detected vessels is not checked. Besides, the threshold selection is also critical. To improve the performance of the conventional matched filter, Rawi *et al.* (2007) proposed an improved matched filter by using an optimizing procedure to search for the best parameters for the method.

Another technique for vessel extraction is the vessel-tracking method (Can *et al.*, 1999; Kochner *et al.*, 1998), in which each vessel segment is defined by three attributes: direction, width, and center point. The density distribution of the cross section of a blood vessel is estimated using a Gaussian shaped function. Individual segments are identified using a search procedure, which keeps track of the center of the vessel and makes some decisions about the future path of the vessel based on certain vessel properties. However, the vessel-tracking method requires a user intervention and may be confused by vessel crossing and bifurcations. To deal with the problem of the central light reflex area in the tracking method, Gao *et al.* (2001) supposed the vessel intensity profiles can be modeled as twin Gaussian functions, and Chutatape *et al.*, (1998) proposed a new method in which the tracking process started from the circumference of the optic disc and applied a Kalman filter as the base to estimate the next search location. Others have proposed the use of pixel classification approaches (Tamura *et al.*, 1983; Cote *et al.*, 1994), which involve two steps. Firstly, a low-level algorithm produces a segmentation of spatially connected regions. These candidate regions are then classified as being vessel or non-vessel. A drawback of these methods is that the large-scale properties of vessels cannot be applied to the classification until the low-level segmentation has already been finished. To overcome the drawback of the pixel classification method, Jorge *et al.*, (2003) presented a novel way by combining multiscale analyzing with supervised classifiers. Recently, some researchers use neural networks (Sinthanayothin *et al.*, 2002) and K-nearest neighbour classifiers (Staal *et al.*, 2004) in vessel segmentation through classifying the retinal image pixels as blood vessel or non-blood vessel pixels. Although the latter three methods can achieve successful experimental results, they are supervised methods and require human interventions. Different manually labeled images will probably lead to different results. In this paper, we present a novel automated hybrid approach for blood vessel extraction using mathematical morphology and a fuzzy clustering algorithm. The method involves two main steps. In the first step, gray mathematical morphology theories are given to smooth and strengthen the retinal images in order to remove the background and enhance the brightness of retinal blood vessels. In the second step, a fuzzy clustering algorithm is employed to extract retinal blood vessels followed by a purification procedure; the final results of the blood vessels are then achieved. The overall data flow of the method is shown in Fig. 1, and detailed information will be explained in what follows. We have compared the performance of our method with the hand-labeled ground truth segmentations and the Hoover method (Hoover *et al.*, 2000) as well as the classical Otsu method (Otsu, 1979). Experimental results on a set of retinal images verify the effectiveness of the proposed method.

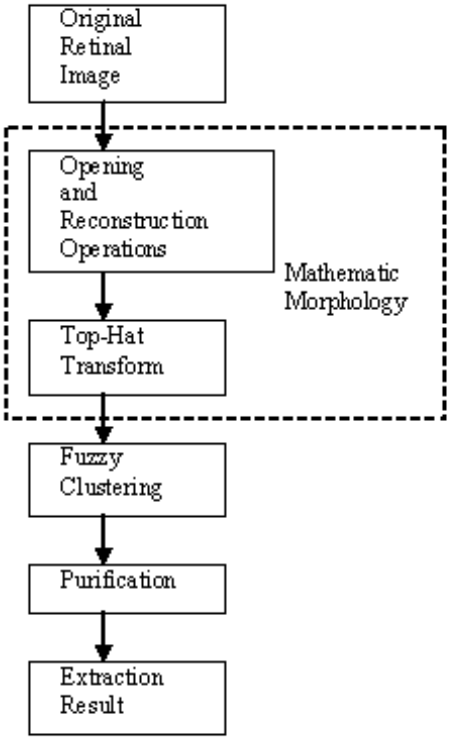


Fig. 1. Flowchart of the proposed technique.

The remainder of this paper is organized as follows: The blood vessels processing procedure based on mathematical morphology is presented in Section 2, and the blood vessels extraction used by the fuzzy clustering algorithm is given in Section 3. Section 4 describes the experimental results and some qualitative and quantitative comparisons. Finally, the conclusions of this paper are drawn in Section 5.

## 2. Blood vessel processing

Retinal images usually have pathological noise and various texture backgrounds, which may cause difficulties in extraction. However, the line type feature of the blood vessels is not changed when the background textures of the image are different. Therefore, as in the previously mentioned references, this paper regards large pathological areas as background textures and only considers small pathological areas for segmentation. Based on this, the outline of our enhancing method is described as follows: Firstly, in order to remove the noise, a gray opening operation and an opening by reconstruction with a linear struc-

turing element are employed to the original image at various orientations. Secondly, the Top-Hat transform combined with reconstruction opening and closing operations are proposed to strengthen the smoothed image by iteratively filtering the image.

**2.1. Smooth image and remove noise.** Gray mathematical morphology theory is a kind of non-linear theory based on set theory and is advantageous to geometrically describe an image (Serra and Soille, 1994). The theory can be used to extract gray linear properties by convolving the image with a line type-structuring element at various orientations (Zana and Klein, 2001)

The key in the gray mathematical morphology process is to select the structuring element. This paper uses linear structuring elements according to the line type property of vessels. However, it is important to note that an opening operation used by a linear structuring element will remove a vessel or some parts of it when the vessels in the image have orthogonal directions or the structuring element is longer than the vessel width. On the contrary, when the structuring element and the vessel have parallel directions, the vessel will never be changed. Therefore, this paper convolves the image with the linear structuring element at various orientations to get the maximum response. To satisfy the need of extracting larger vessels, the length of structuring elements is selected to be close to the diameter value of the largest vessels. In our experiments, in order to save the time spent on the segmentation, the size of the retinal images is now reduced to $221 \times 256 \times 8$, the diameter of the largest vessels is approximately 6 pixels. Hence, each structuring element (every 15) is 7 pixels long and 1 pixel in width.

Structuring elements are applied here to perform an opening operation $\gamma_{L_i}$ on the original image $S_0$. This opening operation consists of two steps. The first step is to erode the image defined as $\varepsilon_L$, and the second step is to dilate the image defined as $\delta_L$. The maximum response of 12 directions is defined as the opened image $S$. The reconstructed image $S_{op}$ that is the smoothed image obtained by carrying out an opening by reconstruction $\gamma_{S_0}^{rec}$ to the original image $S_0$ and the opened image $S$. The calculation process is defined as follows:

$$\gamma_L = \delta_L(\varepsilon_L(M)), \tag{1}$$

$$S = \max_{i=1,\ldots,12}\{\gamma_{L_i}(S_0)\}, \tag{2}$$

$$S_op = \gamma_{S_0}^{rec}(S) = \sup_{d\in N}(\Delta_{S_0}^{d}). \tag{3}$$

Here

$$\varepsilon_L = \min_{M+L(M)}(S_0(M)), \tag{4}$$

$$\delta_L = \max_{M+L(M)}(S_0(M)), \tag{5}$$

$$S_{\Delta_{S_0}^1}^1(S) = \inf(\{\max_{M+C}(S_0(M)), S(M)\}), \tag{6}$$

$$\Delta_{S_0}^{d+1}(S) = \Delta_{S_0}^1(S^d), \tag{7}$$

where $d$ is the calculated time and $C$ is the radius of neighborhood.

Figure 2(a) is an original retinal image. It can be seen that there is a large pathology in the area of fovea and a small pathology in the background. Also, there are a few vessel tumors in the vessels. Before smoothing and removing noise, the color of the original image is reversed. Then, Eqns. (3) and (5) are applied to the reversed image to get the smoothed image. Figure 2(b) is the result of the smoothed image. >From Fig. 2(b), it is easy to see that the noise areas are removed when they are less than the length of structuring elements, whereas the large pathological areas are still preserved as the background.

**2.2. Strengthen vessels and remove background.** After the image has been smoothed, the Top-Hat trans-

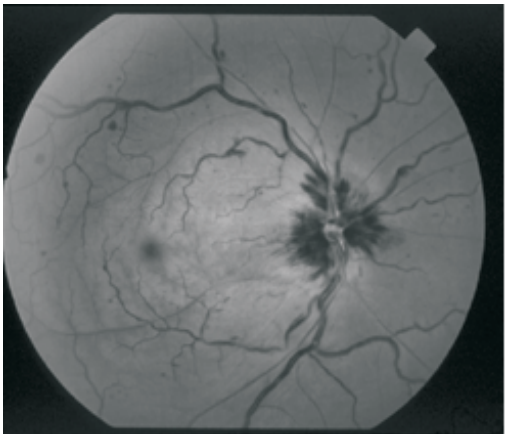

(a)

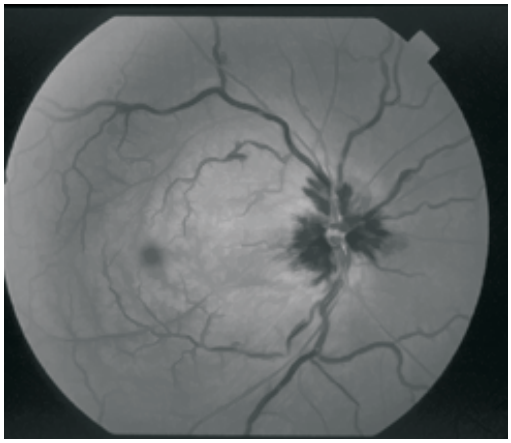

(b)

Fig. 2. Smoothed result of a retinal image: (a) original image, (b) smoothed image.

form is applied to strengthen the vessels in the image by choosing appropriate structuring elements. Here, the Top-Hat transform is applied to the smoothed image at 12 directions, and the computational results of the 12 directions are summed up to increase the gray difference between the vessels and the background. The corresponding formula is as follows:

$$S_{\mathrm{sum}} = \sum_{i=1}^{12} \big(S_{op} - \gamma_{L_i}(S_0)\big). \tag{8}$$

Vessels could be manually segmented with a simple threshold on $S_{\mathrm{sum}}$. However, most images contain noisy data requiring a further treatment. Hence, we continue to smooth the image by a Gaussian filter which is 7 pixels in width, and strengthen the curve feature of vessels by using the Laplacian transform,

$$S_{\mathrm{lap}} = \mathrm{Laplacian}\big(\mathrm{Gaussian}_{\sigma=7/4}^{\mathrm{width}=7}(S_{\mathrm{sum}})\big). \tag{9}$$

Then the operations of opening by reconstruction and closing by reconstruction are applied to the image $S_{\mathrm{lap}}$ to enhance the image iteratively. The size of the structuring elements is still $7 \times 1$ pixels. The opening by reconstruction $\gamma_{S_{\mathrm{lap}}}^{\mathrm{rec}}$ and the closing by reconstruction $\phi_{S_1}^{\mathrm{rec}}$ are respectively defined as

$$S_1 = \gamma_{S_{\mathrm{lap}}}^{\mathrm{rec}}\big(\max_{i=1,\ldots,12}\{\gamma_{L_i}(S_{\mathrm{lap}})\}\big) \tag{10}$$

and

$$S_2 = \phi_{S_1}^{\mathrm{rec}}\big(\min_{i=1,\ldots,12}\{\phi_{L_i}(S_1)\}\big). \tag{11}$$

Here

$$\phi_{S_1}^{\mathrm{rec}} = N_{\max} - \gamma_{(N_{\max}-S_1)}^{\mathrm{rec}}(N_{\max} - S), \tag{12}$$

$$\phi_L(S) = \varepsilon_L(\delta_L(S)), \tag{13}$$

where $N_{\max}$ is the maximum gray level of the original image, and $\phi_L$ is the gray closing operation. Equations (10) and (11) are applied to the previous smoothed image Fig. 2(b) and the result of the strengthened image is shown in Fig. 3. From Fig. 3, we can see the blood vessels have been significantly enhanced and the large pathological area has become one part of the image background. It is important to note that before we can use Eqns. (10) and (11), Eqns. (8) and (9) should be used first.

## 3. Fuzzy clustering for vessel extraction

When the retinal vessels have been enhanced, the next step is to extract the vessels from the image. However, it is important to note there is some ambiguity in determining the exact position of a vessel segment in the image due to the physics of the image-generation process, the individual characteristics of the imaging system and the presence of noise (Ayala *et al.*, 2005). Since fuzzy set theory

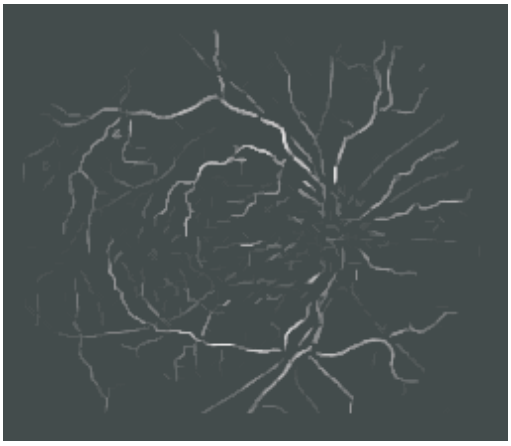

Fig. 3. Enhanced image of Fig. 1(b).

was introduced, it has become a powerful tool to tackle this difficulty in image segmentation. Here, we apply the most popular fuzzy clustering method, i.e., the fuzzy $c$-means (FCM) clustering algorithm to extract the vessels.

The FCM algorithm was first introduced by Dunn (1974) and was later extended by Bezdek (1981). The algorithm is an iterative clustering method that produces an optimal $c$ partition by minimizing the weighted-within-group sum of squared errors $J_{FCM}$ (Bezdek, 1981):

$$J_{FCM} = \sum_{k=1}^{n}\sum_{i=1}^{c}(u_{ik})^q d^2(x_k, v_i), \tag{14}$$

where $X = \{x_1, x_2, \ldots, x_n\} \subseteq \mathbb{R}^p$ is the data set in the $p$-dimensional vector space, $n$ is the number of data items, $c$ is the number of clusters with $2 \le c < n$, $u_{ik}$ is the degree of membership of $x_k$ to the $i$-th cluster, $q$ is a weighting exponent on each fuzzy membership, $v_i$ is the prototype of the centre of cluster $i$, $d^2(x_k, v_i)$ is a distance measure between object $x_k$ and cluster centre $v_i$. A minimum of the objective function $J_{FCM}$ can be obtained via an iterative process, which is as follows:

**Step 1.** Set values of $c$, $q$ and $\varepsilon$.

**Step 2.** Initialize the fuzzy partition matrix $U = [u_{ik}]$.

**Step 3.** Set the loop counter $b = 0$.

**Step 4.** Calculate the $c$ cluster centers $\{v_i^{(b)}\}$ with $U^{(b)}$:

$$v_i^{(b)} = \frac{\sum_{k=1}^{n}(u^{(}b)_{ik})^q x_k}{\sum_{k=1}^{n}(u^{(}b)_{ik})}. \tag{15}$$

**Step 5.** Calculate the membership $U^{(b+1)}$. For $k = 1$ to $n$, calculate the following:

$$I_k = \{i \mid 1 \le i \le c,\, d_{ik} = ||x_k - v_i|| = 0\},$$
$$\widetilde{I} = \{1, 2, \ldots, c\} - I_k.$$

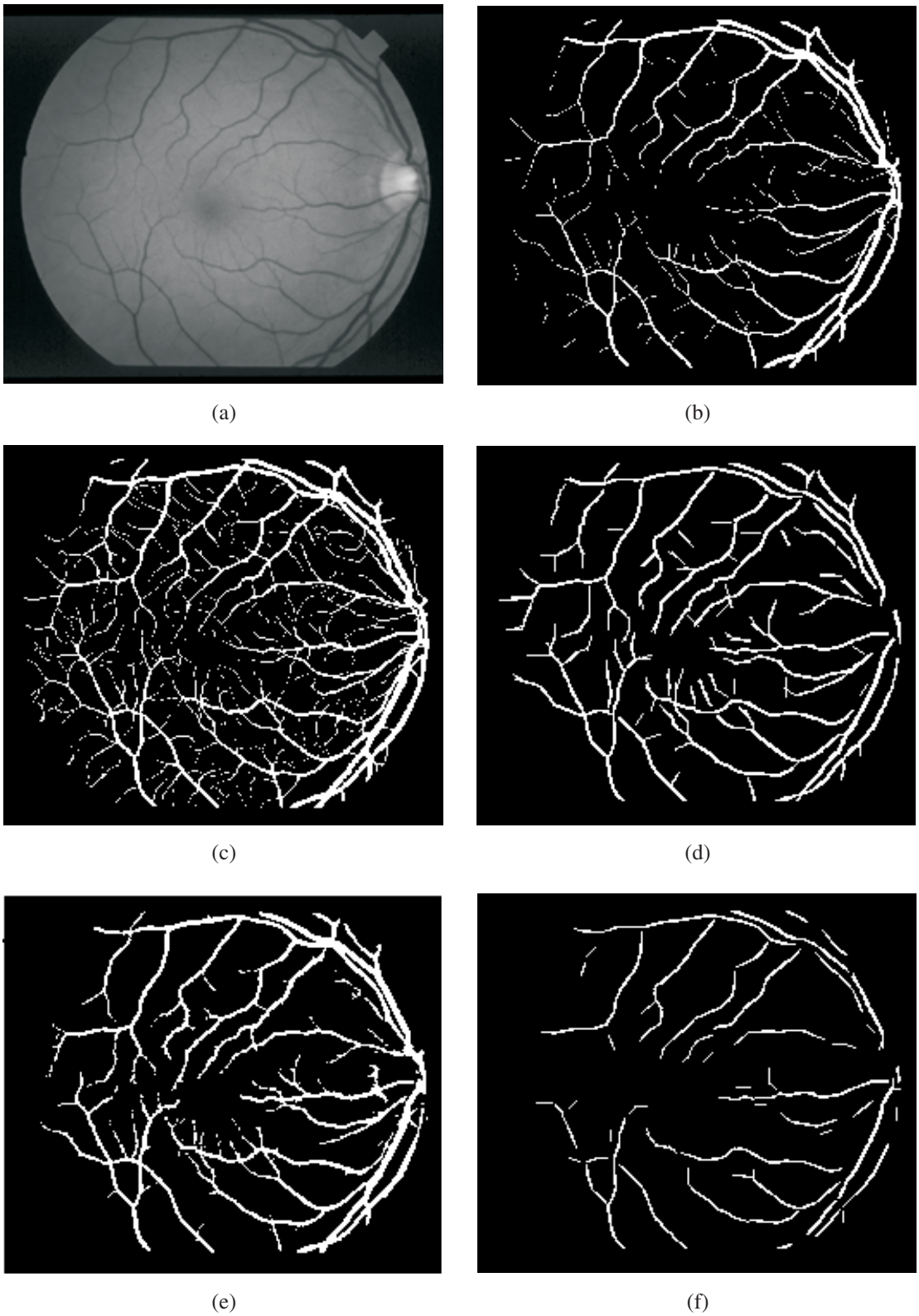

Fig. 4. Results of a normal retinal image: (a) original image, (b) first specialist, (c) second specialist, (d) our method, (e) Hoover's method, (f) Otsu's method.

For the $k$-th column of the matrix, compute new membership values: If $I_k = \phi$, then

$$u_{ik}^{(b+1)} = \frac{1}{\sum_{j=1}^{c} \left(d_{ik}/d_{jk}\right)^{2/(q-1)}}. \quad (16)$$

Otherwise, $u_{ik}^{(b+1)} = 0$ for all $i \in \widetilde{I}_k$ and $\sum_{i \in I_k} u_{ik}^{(b+1)} = 1$. Take next $k$.

**Step. 6** If $||U^(b) - U^{(b-1)}|| < \varepsilon$, stop. Otherwise, set $b = b + 1$ and go to Step 4.

When the algorithm has converged, a defuzzification process takes place in order to convert the fuzzy partition matrix $U$ to a crisp partition. A number of methods have been developed to defuzzify the partition matrix $U$, among which the maximum membership procedure is most important. The procedure assigns object $k$ to class $C$ with the highest membership:

$$C_k = \arg\{\max_i(u_{ik})\}, \quad i = 1, 2, \ldots, c. \quad (17)$$

With this procedure, the fuzzy image is then converted to a crisp one. However, since there are some weak edges and noise in the image after this fuzzy extraction, we then use a purification procedure as in (El-Khamy *et al.*, 2002) to purify the result and the final extraction or segmentation result is achieved in this case.

## 4. Experiments and analysis

In this section, results of applying the proposed approach are presented. In order to test and evaluate the performance of our method, we compare our simulation results with the standard hand-labelled segmentations, which are manually segmented by two eye specialists. Also, the results of the proposed method are compared with those of Hoover *et al.* (2000) and the standard Otsu thresholding method (Otsu, 1979). Here, the Otsu method is applied to the enhanced retinal image instead of the FCM. Since our motivation is to extract the blood vessels from the image, in the FCM algorithm *c* is set to 2. All the experiments are carried out by using the normal or abnormal retinal images, which come from the Hoover database as in the paper by Hoover *et al.* (2000).

Figure 4(a) shows an original normal retinal image. The results produced by the two specialists are given in Figs. 4(b) and (c). Comparing Figs. 4(b) and (c), we can see that the second specialist took a more conservative view of the vessels' boundaries and could identify smaller vessels than the first specialist, which shows that the extraction results depend on the specialist's experience. Therefore, different specialists may achieve different extraction results. This database is available for any interested researcher to develop and evaluate his or her methods. To further evaluate the performance of our approach, the corresponding extraction results used by our method, Hoover's method, and Otsu's method are compared and presented in Figs. 4(d)–(f), respectively.

>From the presented results, it can be seen that Otsu's method produces the worst results out of the three methods. It cannot extract all the blood vessels from the image. Because Otsu's method is a global thresholding method, it relies on the histogram of the image. If the image has no appropriate bi-modal histogram, the method cannot achieve good results. Another important reason is that retinal images usually have very low contrast and with much ambiguity the images then have indistinguishable histograms but no bi-modal histogram. Therefore, the classical Otsu thresholding technique cannot easily find a criterion of similarity or closeness for thresholding, which consequently leads to bad segmentation results. On the other hand, comparing Figs. 4(d) and (e), we can find that our method can give a virtually identical result to that of Hoover and the two methods perform better than Otsu's method. However, it is important to note that the Hoover method depends on the threshold, and different thresholds perhaps will yield different results, while our method is almost fully automatic.

The second example is an abnormal retinal image with a large pathological area, as shown in Fig. 5(a). We apply the proposed method, Hoover's method, and Otsu's method to the image, and the corresponding results are given in Figs. 5(b)–(d), respectively. From the results, it is easy to see that even if the retinal image has a large pathological area, Hoover's and our method can still automatically extract the vessels correctly from the image. However, Otsu's method cannot yet accurately segment the vessels from the retinal image.

Finally, we carried out a series of experiments on twenty normal and abnormal retinal images from Hoover's database to further test quantitatively the performance of the proposed approach. To measure the segmentation accuracy, the true positive rate $P_{\text{true}}$ and the false positive rate $P_{\text{false}}$ are introduced as

$$P_{\text{true}} = \frac{\text{TrueNum}}{\text{Num}_{vp}}, \quad (18)$$

$$P_{\text{false}} = \frac{\text{FalseNum}}{\text{Num}_{uvp}}, \quad (19)$$

where $\text{Num}_{vp}$ is the sum of the pixels that are marked as a vessel in a ground actual image, $\text{Num}_{uvp}$ is the sum of the pixels that are marked as non-vessel in the ground actual image, $\text{TrueNum}$ is the sum of the pixels that are segmented as vessel truly, and $\text{FalseNum}$ is the sum of the pixels that are segmented as vessel falsely. Here, the results of the first observer are considered as the ground truth as in (Can *et al.*, 1999). Figure 6(a) shows the true positive rates of our method with the second specialist's

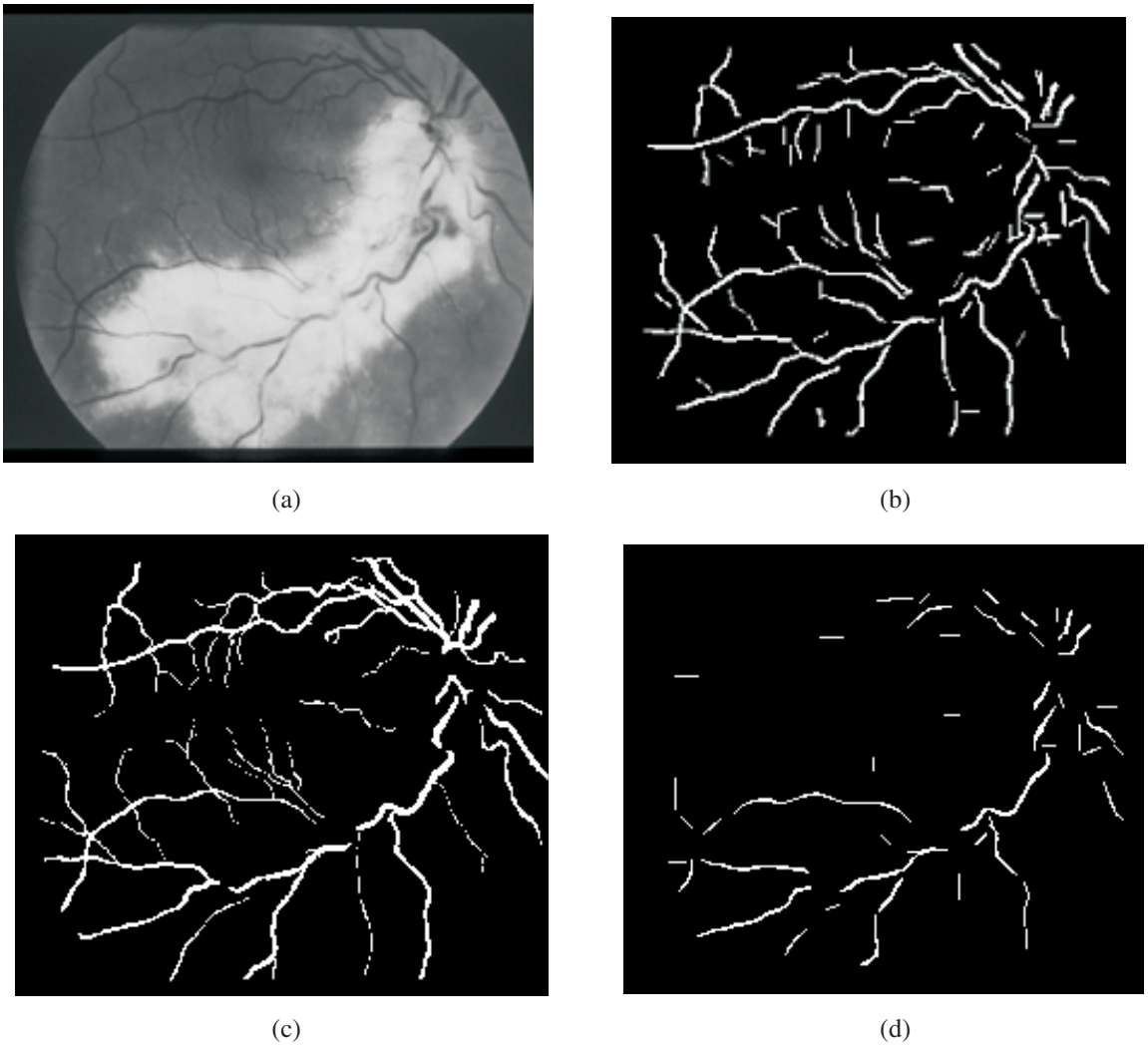

(a) (b)

(c) (d)

Fig. 5. Results of an abnormal retinal image: (a) original image, (b) our method, (c) Hoover's method, (d) Otsu's method.

segmentations, and Fig. 6(b) shows the false positive rates of our method with the second specialist's segmentations. Based on the results, we can conclude that our method can produce true positive rates in much the same way as the second specialist. However, the false positive rates of our method are less than those of the second specialist, which means that our method can yield smaller vessels than the second specialist. The results presented here demonstrate the our method can produce comparable results to the ground truth, which indicates that the proposed automated method is effective.

## 5. Conclusions

In this paper, a novel automatic hybrid method for the extraction of retinal image vessels is presented. The method is developed by using mathematical morphology combined with the fuzzy clustering algorithm. Mathematical morphology is first employed to smooth and strengthen the retinal images as well as to suppress the background information. Then, the fuzzy clustering algorithm is applied to the enhanced retinal images. Finally, a purification procedure is introduced to the fuzzy segmentation results. The blood vessels are then extracted. The detection results obtained from the proposed method are compared with those of the standard manual ground truth segmentations and some other segmentation methods. Both qualitative and quantitative experiments on normal and abnormal retinal images indicate that the proposed approach is effective and can produce identical results as the ground truth and yield a higher accuracy ratio and a lower misclassification ratio than the manual extractions.

## Acknowledgements

The authors wish to thank the anonymous referees for their valuable suggestions. This work is supported by

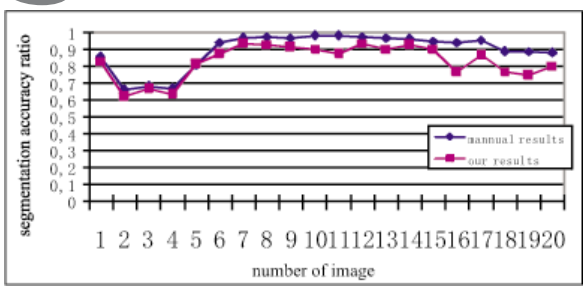


(a)

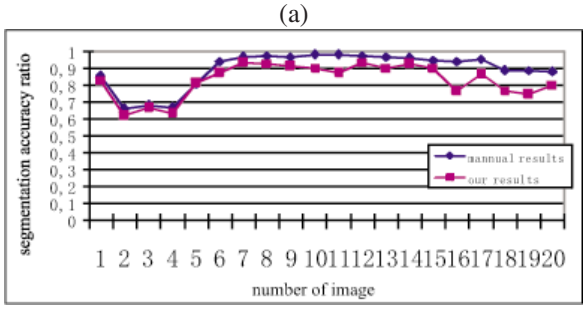


(b)

Fig. 6. Comparisons of extraction results: (a) accuracy ratio, (b) misclassification ratio.

the China Postdoctoral Science Foundation funded project under the grant no. 20080431277, and the Science and Technology Research Project of the Education Department of Jiangxi Province under the grant no. 2007-270.

## References

Ayala G., Leon T. and Zapater V. (2005). Different averages of a fuzzy set with an application to vessel segmentation, *IEEE Transactions on Fuzzy Systems* **13**(3): 384–393.

Bezdek J.C.(1981). *Pattern Recognition with Fuzzy Objective Function Algorithms*, Plenum Press, New York, NY.

Can A., Shen H., Turner J.N., Tanenbaum H.L., and Roysam D. B. (1999). Rapid automated tracing and feature extraction from retinal fundus images using direct exploratory algorithms. *IEEE Transactions on Information Technology in Biomedicine* **3**(2): 125-138.

Chanwimaluang T. and Fan G. (2003). An efficient blood vessel detection algorithm for retinal images using local entropy thresholding, *Proceedings of IEEE International Symposium on Circuits and Systems*, Bangkok, Thailand, Vol. 5, pp. 21–24.

Chaudhuri S., Chatterjee S., Katz N., Nelson M. and Goldbaum M. (1989). Detection of blood vessels in retinal images using two-dimensional matched filters, *IEEE Transactions on Medical Imaging* **8**(3): 263–269.

Chutatape O., Zheng L. and Krishnan S. M. (1998). Retinal blood vessel detection and tracking by matched Gaussian and Kalman filters, *Proceedings of the IEEE Conference on Engineering in Medicine and Biology, Hong Kong, China*, Vol. 6, pp. 3144–3149.

Chutatape O., Zheng L. and Krishnan S. M. (1998). Retinal blood vessel detection and tracking by matched Gaussian and Kalman filters, *Proceedings of the IEEE Conference on Engineering in Medicine and Biology, Hong Kong, China*, Vol. 6, pp. 3144–3149.

Cote B., Hart W., Goldbaum M., Kube P. and Nelson M. (1994). *Classification of blood vessels in ocular fundus images,* Technical report, University of California, San Diego, CA.

Dunn J.C. (1973). A fuzzy relative of the ISODATA process and its use in detecting compact well separated clusters, *Journal of Cybernetics* **3**(3): 32–57.

EI-Khamy S. E., Ghaleb I. and EI-Yamany N. A. (2002). Fuzzy edge detection with minimum fuzzy entropy criterion, *Proceedings of the Mediterranean Electrotechnical Conference, Cairo, Egypt*, 1: 498–503.

Gao X. H., Bharath A., Stanton A., Hughes A., Chapman N. and Thom S. (2001). A method of vessel tracking for vessel diameter measurement on retinal images, *Proceedings of IEEE International Conference on Image Processing,* Thessaloniki, Greece, Vol. 2, pp. 881–884.

Hoover A., Kouznetsova V. and Goldbaum M. (2000). Locating blood vessels in retinal images by piecewise threshold probing of a matched filter response, *IEEE Transactions on Medical Imaging,* **19**(3): 203–210.

Jorge J. G. L., Joao V. B. S., Roberto M. C. J. and Herbert F. J. (2003). Blood vessels segmentation in non-mydriatic images using wavelets and statistical classifiers, *Proceedings of Brazilian Symposium on Computer Graphics and Image Processing,* Sao Carlos, Brazil, 1: pp. 262–269.

Kochner B., Schulmann D., Michaelis M., Mann G. and Englemeier K. H. (1998). Course tracking and contour extraction of retinal vessels from colour fundus photographs: Most efficient use of steerable filters for model based image analysis, *SPIE Proceedings of Medical Imaging* **3328**(2): 755–761.

Otsu N. (1979). A threshold selection method from gray level histogram, *IEEE Transactions on Systems, Man, and Cybernetics* **9**(1): 62–66.

Rawi M. A., Qutaishat M. and Arrar M. (2007). An improved matched filter for blood vessel detection of digital retinal images, *Computers in Biology and Medicine* **37**(2): 262–267.

Riveron E. F. and Guimeras N. G. (2006). Extraction of blood vessels in ophthalmic color images of human retinas, *Lecture Notes in Computer Science,* **4225**: 118–126.

Serra J. and Soille P. (1994). *Mathematical Morphology and Its Applications to Image Processing*, Kluwer Academic Publishers, Boston, MA.

Sinthanayothin C., Boyee J.F., Williamson T.H., Cook H.L., Mensah E., Lal S. and Usher D. (2002). Automatic detection of diabetic retinopathy on digital fundus images, *Diabetic Medicine* **19**(2): 105–112.

Staal J., Abramoff M.D., Niemeijer M., Viergever M.A. and Ginneken B. V. (2004). Ridge-based vessel segmentation in color images of the retina, *IEEE Transactions on Medical Imaging* **23**(4): 501–509.

Stapor K., Switonski A., Chrastek R. and Michelson G. (2004). Segmentation of fundus eye images using methods of mathematical morphology for glaucoma diagnosis, *Lecture Notes in Computer Science,* **3039**: 41–48.

Stapor K. and Switonski A. (2004). Automatic analysis of fundus eye images using mathematical morphology and neural networks for supporting glaucoma diagnosis, *Machine Graphics & Vision* **13**(1/2): 65–78.

Tamura S., Tanaka K., Ohmori S., Okazaki K., Okada A. and Hoshi M. (1983). Semiautomatic leakage analyzing system for time series fluorescein ocular fundus angiography, *Pattern Recognition* **16**(1): 149–162.

Zana F. and Klein J.C. (2001). Segmentation of vessel-like patterns using mathematical morphology and curvature evaluation, *IEEE Transactions on Image Processing* **10**(7): 1010–1019.

Received: 19 September 2007
Revised: 26 January 2008
Re-revised: 7 April 2008